ELIMINATION OF DEAD-VOLUME CONTRIBUTIONS TO MOMENTS OF CHROMATOGRAPHIC PEAKS

Helena DAVIDOVÁ and Petr SCHNEIDER

Institute of Chemical Process Fundamentals, Czechoslovak Academy of Sciences. 165 02 Prague 6-Suchdol

Received January 12, 1989
Accepted February 6, 1989

Dedicated to late Academician Eduard Hála.

Two methods for correction of moments of peaks from packed columns were applied to experimental responses of columns packed with porous γ-alumina in the shape of Raschig rings: 1. subtraction of moments for columns of two lengths and 2. application of dead volume corrections obtained by independent measurements. It appears that both methods give identical results. An advantage of the second methods lies in increased accuracy and decreased amount of necessary measurements.

The shape of a peak which appears at the outlet of a column filled with porous packing, as a response to injection of gaseous tracer into the stream of carrier gas, contains information on all processes which take place inside the column. Analysis of the peak-shape can, thus, at least in principle, provide simultaneously adsorption rate and equilibrium constants for tracer adsorption on the internal surface of column packing, effective diffusion coefficient of the tracer in the pores of packing, mass transfer coefficient for tracer (transport between the outer surface of packing particles and bulk gas) and axial dispersion coefficient which characterizes axial and radial mixing in the flowing carrier gas[1-3]. In practice, however, parameters characterizing only a subset of these processes are looked for; a frequent choice is the adsorption equilibrium constant and effective diffusivity.

The peak-shape analysis can be performed basically in three ways: *1*) by matching response peaks, obtained by numerical solution of the governing (partial differential) mass balance equations which describe the processes in the column, to experimental peaks in the time domain (e.g. ref.[4]), *2*) by similar matching performed, however, in some transformation domain (e.g. in Laplace or Fourier domain[5,6]) and *3*) by matching moments of experimental response curves to expressions which can be developed from the Laplace image of solution of the material balance equations (e.g. refs[1-3,7]).

Whereas matching in time or transformation domains requires sophisticated numerical techniques both for integration of differential equations and parameter

searching, the application of the moment method is quite simple. Because of its straightforwardness the moment method is popular and frequently used; owing to the uncertainty in tail parts of response peaks, which is magnified during determination of higher moments, usually only the first ordinary (μ_1') and the second central (μ_2) moments are utilized. For a response signal $c(t)$ the moments are defined in the following way

$$\mu_1' = m_1/m_0 \tag{1}$$

$$\mu_2 = m_2/m_0 - (\mu_1')^2 , \tag{2}$$

where m_i ($i = 1, 2$) are integrals of the response signal

$$m_0 = \int_0^\infty c(t)\,\mathrm{d}t\,; \quad m_1 = \int_0^\infty t\,c(t)\,\mathrm{d}t\,; \quad m_2 = \int_0^\infty t^2\,c(t)\,\mathrm{d}t\,. \tag{3}$$

Theoretical expressions are available for moments of impulse response curves, i.e. for responses of the packed column to inlet disturbance in the shape of Dirac peak, $\bar{\mu}_1'$, $\bar{\mu}_2$ (e.g. refs[1-3,7]). Moments of an experimental peak μ_1', μ_2 are, however, larger than the impulse response moments $\bar{\mu}_1'$, $\bar{\mu}_2$ because they include also contributions due to the width of the actual inlet disturbance, $(\mu_1')_0$, $(\mu_2)_0$, and due to processes which take place inside the connecting gas lines and fitting elements between the upstream tracer injection point and downstream detector $(\mu_1')_d$, $(\mu_2)_d$. Sometimes the packed column is divided into several sections; moment contributions of the connecting gas lines and fittings between these sections must be also included in $(\mu_1')_d$, $(\mu_2)_d$. Thus,

$$\mu_1' = \bar{\mu}_1' + (\mu_1')_0 + (\mu_1')_d\,, \tag{4}$$

$$\mu_2 = \bar{\mu}_2 + (\mu_2)_0 + (\mu_2)_d\,. \tag{5}$$

For a rectangular inlet concentration pulse of width t_0 it follows from Eqs (*1*)–(*3*) that moments $(\mu_1')_0$, $(\mu_2)_0$ are given as

$$(\mu_1')_0 = t_0/2\,, \tag{6}$$

$$(\mu_2)_0 = t_0^2/12\,. \tag{7}$$

It is, however, difficult to verify whether the actual shape of the inlet pulse in experiments can be approximated in this way. Even less is known about the magnitude of moment contributions due to dead-spaces $(\mu_1')_d$, $(\mu_2)_d$. This is a serious drawback because often moment contributions $(\mu_1')_0$, $(\mu_2)_0$ and $(\mu_1')_d$, $(\mu_2)_d$ represent a significant part of μ_1' and or μ_2. Such a situation is encountered always when nonadsorbable tracers are used together with high velocities of carrier gases, i.e. under conditions

which are favourable for decreasing the influence of axial dispersion, external mass transfer and surface transport.

It is the aim of this paper to compare two approaches for elimination of moment contributions $(\mu_1')_0$, $(\mu_2)_0$, $(\mu_1')_d$ and $(\mu_2)_d$ from moments of experimental column response signals μ_1' and μ_2 and, thus, for obtaining the moments of impulse response signal $\bar{\mu}_1'$, $\bar{\mu}_2$.

The first method subtracts moments of experimental response signals determined independently for two column lengths, L_1, L_2, (i.e. $\mu_1'(L_1) - \mu_1'(L_2)$ and $\mu_2(L_1) - \mu_2(L_2)$) with the same arrangement of elements connecting the columns.

$$\bar{\mu}_1'(L_1 - L_2) = \mu_1'(L_1) - \mu_1'(L_2)\,, \tag{8}$$

$$\bar{\mu}_2(L_1 - L_2) = \mu_2(L_1) - \mu_2(L_2)\,. \tag{9}$$

Relations (*8*) and (*9*) follow from the direct proportionality between moments and length of the column packing[1-3,9]: $\mu_1' \sim L$, $\mu_2 \sim L$.

The second method corrects moments of experimental responses determined for one column length, L, by subtraction of independently determined moments for the experimental setup with removed columns, $(\mu_1')_d + (\mu_1')_0 \equiv (\mu_1')_{0d}$ and $(\mu_2)_d + (\mu_2)_0 \equiv (\mu_2)_{0d}$

$$\bar{\mu}_1'(L) = \mu_1'(L) - (\mu_1')_{0d}\,, \tag{10}$$

$$\bar{\mu}_2(L) = \mu_2(L) - (\mu_2)_{0d}\,. \tag{11}$$

Illustration of these procedures is based on experimental data obtained during a study of effective diffusion coefficients of simple gases at laboratory conditions in porous Raschig rings formed from γ-alumina.

EXPERIMENTAL

γ-Alumina Raschig rings (o.d. 4·8 mm, i.d. 1·9 mm, height 4·2 mm). Textural properties are summarized in Table I.

Gases. Hydrogen and nitrogen were used as carrier gases, hydrogen, helium, and nitrogen as tracers.

Columns were arranged from pieces of straight copper tubing (o.d. 6 mm, i.d. 2·49 mm, length 55 cm or 27·5 cm) connected in series by short rubber capillaries (i.d. 2 mm). Raschig rings were slid one by one on a straight copper wire (diameter 1·9 mm) which completely filled the central holes of Rashig rings; in this way an (nearly) infinite cylindrical geometry was achieved. The wire with pellets was placed axially in the copper tube, leaving only a narrow concentric free space between the outer surface of pellets and internal surface of the tube (width approx. 0·1 mm). On the top and bottom of this packing special nonporous pieces were inserted which served for distribution of the carrier gas stream and fixing the wire with Raschig rings. Rubber

stoppers with short piece of centrally placed metallic capillary closed the tubes from both sides and fastened firmly the packing. Details of the column arrangement are sketched in Fig. 1. By connecting four packed tubes (length 55 cm or 27·5 cm) in series, two columns (with packing lengths 211·8 cm and 101·3 cm) were set up.

For measurements of response peaks corresponding to spaces outside the packed tube parts and to tube connections, the 55 cm and 27·5 cm packed tubes were replaced by identical copper tubes with length equal to twice the height of the nonporous terminal distribution/fixing pieces.

Apparatus. For regulation of carrier gas flow rates mass flow regulator, calibrated with a soap-film meter, was employed. Tracer gases were introduced into the carrier gas stream from a sampling loop (volume 1·14 cm^3) connected to a six port valve. Near the column inlet a mercury filled U-manometer was connected for monitoring the pressure drop across the column. For analysis of the outlet stream from the column a thermal conductivity detector was used. The

TABLE I

Textural properties of Raschig rings

Specific surface[a]	205 m^2/g
Apparent density[b]	1·074 g/cm^3
True (skeletal) density[c]	3·182 g/cm^3
Pore volume[d]	0·617 cm^3/g
Porosity[e]	0·662
Most frequent macropore radius[f]	123 nm
Most frequent mesopore radius[f]	3 nm

[a] BET; [b] ϱ_p pycnometrically with mercury; [c] ϱ pycnometrically with helium (AutoPycnometer 1320, Micromeritics, U.S.A.); [d] $V_p = (1/\varrho_p) - (1/\varrho)$; [e] $\varepsilon = 1 - (\varrho/\varrho_p)$; [f] mercury porosimetry (AutoPore 9200, Micromeritics, U.S.A.).

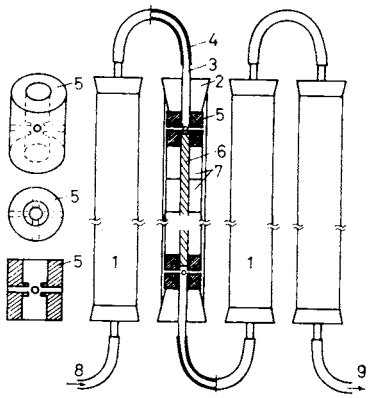

FIG. 1

Sketch of packed columns and connection elements. **1** Column, **2** rubber stopper, **3** stainless steel capillary, **4** rubber tubing, **5** distribution/fixing pieces, **6** copper wire, **7** γ-alumina pellets (Raschig rings), **8** from sampling valve, **9** to thermal conductivity detector

time dependent concentration signal from this detector was fed into a digital regulator/computer which logged 2 000 concentration points uniformly distributed over the significant time interval. Moments μ_1', μ_2 of experimental response signals were determined numerically (Simpson's rule), according to definitions (*1*)–(*3*), from the stored data.

RESULTS AND DISCUSSION

Pressure Drop Correction

Moments of experimental response peaks for injection of hydrogen into the stream of nitrogen (H → N)* for the long column (L_1 = 211·8 cm) are plotted in Figs 2 and 3 versus reciprocal linear nitrogen velocity $1/v_e$, calculated for conditions at the column exit ($v_e = F_e/S$; F_e is the volumetric carrier gas flow rate at conditions of the column exit, S represents the column free cross-section). It can be seen that the dependences do not pass through the origin of coordinates. This is caused by neglecting the pressure drop across the column[8]; due to the increased pressure in upstream column parts, the mean carrier gas velocity is lower than at the column exit. To take this effect into account it is necessary to apply correction factors f_1 and f_2

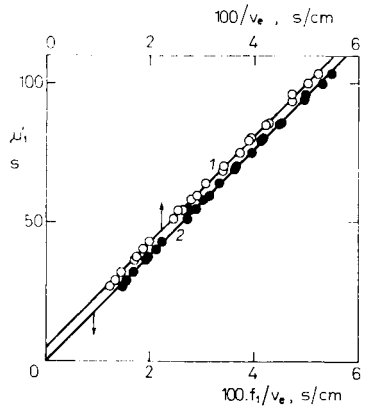

FIG. 2

μ_1' versus $1/v_e$ and f_1/v_e for H→N and column length 211·8 cm. *1* No correction for pressure drop ($1/v_e$), *2* corrected for pressure drop (f_1/v_e)

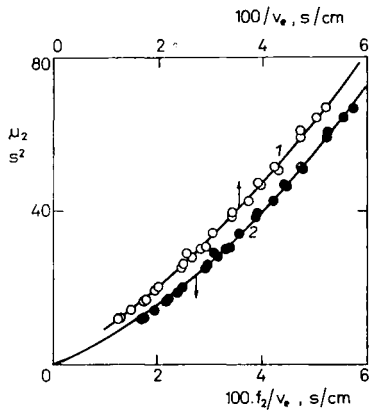

FIG. 3

μ_2 versus $1/v_e$ and f_2/v_e for H→N and column length 211·8 cm. *1* No correction for pressure drop ($1/v_e$), *2* corrected for pressure drop (f_2/v_e)

* In the following text, the injection of tracer gas A into carrier gas B will be denoted as A → B.

for correlations of μ_1' and μ_2, respectively, defined as[9]

$$f_1 = \frac{2}{3}\frac{p^3 - 1}{p^2 - 1}, \tag{12}$$

$$f_2 = \frac{1}{2}\frac{p^4 - 1}{p^2 - 1}, \tag{13}$$

where p denotes the ratio of pressures at the column inlet, p_i, and exit, p_e, respectively, i.e. $p \equiv p_i/p_e$. Plots of moments versus reciprocals of corrected carrier gas velocities v_e/f_1 and v_e/f_2, in Figs 2 and 3, pass through the origin as required.

Measurements of $\bar{\mu}_1'$ and $\bar{\mu}_2$ with Two Column Lengths

Dependences of moments for column lengths $L_1 = 211{\cdot}8$ cm and $L_2 = 101{\cdot}3$ cm on pressure corrected reciprocal carrier gas velocities are illustrated in Figs 4 and 5 for systems H → N and N → H.

Linear regression of the μ_1' data

$$\mu_1'(L) = a(L)(f_1/v_e) \tag{14}$$

gave for N → H: $a(211{\cdot}8\text{ cm}) = 2\,348$ cm (standard deviation ± 17) and $a(101{\cdot}3\text{ cm}) = 1\,192 \pm 15$ cm. Thus, $a(L_1 - L_2) = 1\,156 \pm 32$ cm, where $L_1 - L_2 = 110{\cdot}5$ cm

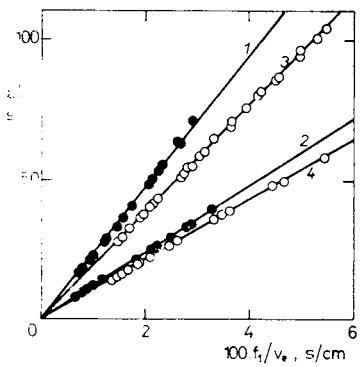

FIG. 4

μ_1' for N → H (●) and H → N (○). Column length: *1*, 211·8 cm; *2*, 101·3 cm

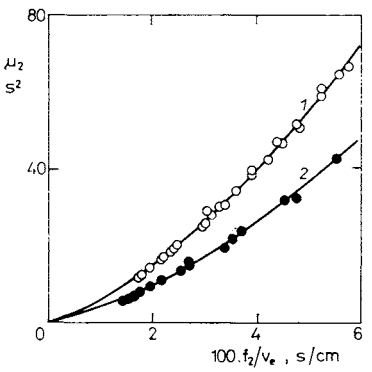

FIG. 5

μ_2 for H → N. Column length: *1* 211·8 cm; *2* 101·3 cm

and the first ordinary moment of the impulse response signal $\bar{\mu}_1'$ for packing length $L = 110{\cdot}5$ cm can be expressed as $\bar{\mu}_1' = (1\,156 \pm 32)(f_1/v_e)$. Then, the first ordinary moment of the impulse response signal per unit column packing length $\bar{M}_1'$ ($\bar{M}_1' \equiv \bar{\mu}_1'/L$) can be represented as

$$\bar{M}_1' = A(f_1/v_e) \tag{15}$$

with $A = 10{\cdot}46 \pm 0{\cdot}29$.

Similarly, for H → N, $a(211{\cdot}8\text{ cm}) - a(101{\cdot}3\text{ cm}) = a(110{\cdot}5\text{ cm}) = (1\,914 \pm 7) - (1\,074 \pm 9) = (841 \pm 15)$ cm and $\bar{\mu}_1'$ $(110{\cdot}5\text{ cm}) = (841 \pm 16)(f_1/v_e)$ from which $A = 7{\cdot}61 \pm 0{\cdot}14$.

The results for other tracer-carrier gas pairs (A → B) are summarized in Table II. It can be seen that adsorption of nitrogen tracer is slightly higher than of hydrogen tracer; this causes longer retention of nitrogen in the column at comparable carrier gas velocities.

The experimental pairs $\mu_2 - f_2/v_e$ illustrated in Fig. 5 were correlated as

$$\mu_2 = b(f_2/v_e) + c(f_2/v_e)^2 . \tag{16}$$

From least-squares analysis of the H → N data for both column lengths L_1, L_2 it follows that $b(211{\cdot}8\text{ cm}) - b(101{\cdot}3\text{ cm}) = b(110{\cdot}5\text{ cm}) = (558{\cdot}7 \pm 28) - (329{\cdot}6 \pm 24) = (229{\cdot}1 \pm 52)$ cm s. Coefficients of quadratic terms, c, are similar for both column lengths: $c(211{\cdot}8\text{ cm}) = 10\,971 \pm 998\text{ cm}^2$; $c(101{\cdot}3\text{ cm}) = 9\,500 \pm 834\text{ cm}^2$. When standard deviations of c's are taken into account it is seen that these coefficients cancel out. Thus $\bar{\mu}_2 = (229{\cdot}1 \pm 52)(f_2/v_e)$ and the dependence of second central moment of the impulse response signal per unit packing length, M_2, on f_2/v_e can be described as

$$\bar{M}_2 = B(f_2/v_e) \tag{17}$$

with $B = 2{\cdot}07 \pm 0{\cdot}29$ s. Results for other A → B systems are summarized in Table III.

Independent Dead-Volume Corrections

First ordinary and second central moments of response peaks determined for connection tubing, inlet and outlet sections of columns (i.e. for columns with $L = 0$) and tracer sampling valve, $(\mu_1')_{0d}$, $(\mu_2)_{0d}$, are shown in Figs 6 and 7. For five gas pairs, A → B, dead-volume moments are split into two groups: for the first moment data with nitrogen carrier gas (i.e. H → N, He → N) fall into one group and data with helium or hydrogen as carrier gases (i.e. N → H, N → He, He → H) fall into another group. For the second moment the groups are similar, except for the He → H

gas system which now falls into the group where data for nitrogen carrier gas are present.

Reciprocal volumetric flow rates at conditions of the system exit, $1/F_e$ or $1/F_e^2$, are used as independent variables. No pressure drop correction is required because pressure drops are negligible in these cases.

The first moment data can be expressed as

$$(\mu_1')_{0d} = \alpha(1/F_e) \tag{18}$$

with $\alpha = 4{\cdot}50 \pm 0{\cdot}02$ cm^3 for He → N and H → N and $\alpha = 4{\cdot}02 \pm 0{\cdot}02$ cm^3 for N → H, N'→ He and He → H. Difference between the two α's is not large (about 10%) but it is statistically significant. As α represents the sum of volumes of con-

TABLE II

First ordinary moments of the impulse response signal

A → B	a^a, cm	A^b	A'^c
H → N	841 ± 16[d]	7·61 ± 0·14	7·71 ± 0·02
He → H	1 004 ± 47	9·08 ± 0·50	8·63 ± 0·09
He → N	875 ± 34	7·92 ± 0·35	8·17 ± 0·08
N → H	1 156 ± 32	10·46 ± 0·29	10·00 ± 0·05
N → He	885 ± 25	8·00 ± 0·24	8·48 ± 0·04

[a] For $L_1 - L_2 = 110{\cdot}5$ cm; [b] from subtraction of μ_1' for two column lengths; [c] corrected by $(\mu_1')_{0d}$; [d] standard deviation.

TABLE III

Second central moments of the impulse response signal

A → B	b^a, cm s	B^b, s	B'^c, s
H → N	229·1 ± 52[d]	2·07 ± 0·25	2·64 ± 0·13
He → N	161·0 ± 138	1·46 ± 1·25	2·46 ± 0·41
He → N	146·8 ± 93	1·33 ± 0·84	1·74 ± 0·31
N → H	347·5 ± 96	3·14 ± 0·87	3·55 ± 0·21
N → He	284·2 ± 95	2·57 ± 0·86	2·80 ± 0·17

[a] For $L_1 - L_2 = 110{\cdot}5$ cm; [b] from subtraction of μ_2 for two column lengths; [c] corrected by $(\mu_2)_{0d}$; [d] standard deviation.

nection elements and one half of the volume of tracer sampling loop (see Eq. (6)) it follows that the volume of connection elements lies around 3·5 – 4·0 cm³.

Second central moments $(\mu_2)_{0d}$ can be correlated as

$$(\mu_2)_{0d} = \gamma(1/F_e^2) \tag{19}$$

with $\gamma = 1{\cdot}57 \pm 0{\cdot}01$ cm⁶ for He → H, He → N and H → N and $\gamma = 0{\cdot}89 \pm 0{\cdot}01$ cm⁶ for N → H and N → He. Similarly as with $(\mu_1')_{0d}$ these values are statistically significantly different. Taking into account Eq. (7), the volumes in which mixing takes place, with simultaneous peak spreading, amount to 0·9 – 1·2 cm³.

By subtracting appropriate correlation $(\mu_1')_{0d} = \alpha(1/F_e)$ (with F_e replaced by v_eS) from dependences $\mu_1' = a(f_1/v_e)$ for all gas pairs and both column lengths, first moments of impulse response signals, $\bar{\mu}_1'$, can be obtained. These moments, converted to unit packing, $\bar{M}_1'$, are given as

$$\bar{M}_1' = A'(f_1/v_e)\,. \tag{20}$$

Coefficients A' are shown in Table II.

For correction of second central moments of experimental response signals, μ_2, it is of importance that correlations of $(\mu_2)_{0d}$ contain only terms with $(1/F_e)^2$; terms with $(1/F_e)$ are not present. If the volumetric flow rate in $\gamma(1/F_e^2)$ is replaced by v_e ($F_e = v_eS$) it follows that the quadratic contributions in μ_2 correlations (5), $c(f_2/v_e)^2$, are wholly due to dead-volume effects. Thus, second central moments of impulse response signals, $\bar{\mu}_2$, are simply $\bar{\mu}_2 = b(f_2/v_e)$; i.e. they are described by

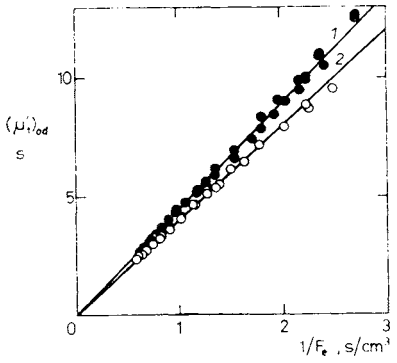

FIG. 6

$(\mu_1')_{0d}$ versus $1/F_e$. *1* He → N, H → N; *2* N → H, N → He, He → H

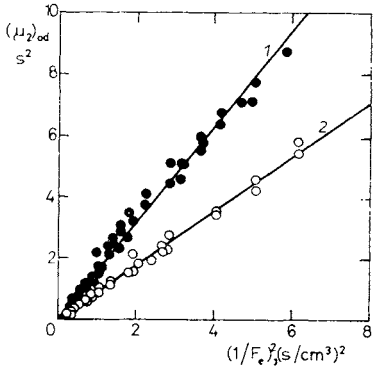

FIG. 7

$(\mu_2)_{0d}$ versus $1/F_e^2$. *1* He → H, He → N, H → N; *2* N → H, N → He

Eq. (5) with the second terms on right-hand side neglected. Second moments of impulse response signals per unit packing length, $\overline{M}_2$, can be, thus, given as

$$\overline{M}_2 = B'(f_2/v_e) . \qquad (21)$$

Coefficients B' are summarized for all tracer – carier gas pairs in Table III.

Comparison of Both Methods for Moments Correction

Coefficients A and A' which characterize first ordinary moments of impulse response signals (cf. Eqs (15), (20)) are compared in Table II. When the confidence intervals of A and A' are taken into account it is obvious that both correction methods give identical results. It seems, however, that the use of separately determined corrections $(\mu_1')_{0d}$ results in smaller spread of coefficients A' than subtraction of results for two column lengths.

Similar situation is with correction of second central moments of experimental response signals: whereas the confidence intervals of B and B' (cf. Eqs (17) and (21)) overlap, the accuracy of B' is clearly better.

Thus, it seems that both compared methods for obtaining moments of impulse response signals from moments of experimental response peaks give essentially identical results and there is, therefore, no reason for preferring one method against the other. One argument can be presented in favor of using independently measured moments $(\mu_1')_{0d}$, $(\mu_2)_{0d}$, viz. the better accuracy resulting in narrower confidence intervals of A' and B'. This method is also less demanding as far as the experimental effort is concerned; whereas subtraction of moments for two column lengths requires doubled measurements for each column packing, determination of $(\mu_1')_{0d}$ and $(\mu_2)_{0d}$ does not depend on the porous samples with which the column will be packed.

LIST OF SYMBOLS

a, b, c	regression coefficients
A, A', B, B'	proportionality constants
$c(t)$	response signal
f_1, f_2	pressure correction factors
F_c	volumetric flow rate of carrier gas at column outlet conditions
L, L_1, L_2	column packing length
$m_i (i = 0, 1, 2)$	integrals (Eq. (3))
p	relative pressure ($p = p_i/p_c$)
p_i, p_c	pressure at column inlet and outlet, respectively
S	column free cross section
t	time from the moment of tracer injection
t_0	width of the injected square wave pulse
v_e	linear velocity of carrier gas in the interparticle space of column packing at conditions of column outlet

$\bar{M}_1'$, $\bar{M}_2$	first ordinary and second central moments of impulse response signal per unit packing length, respectively
α, β, γ	regression coefficients
μ_1', μ_2	first ordinary and second central moments of response signal
$\bar{\mu}_1'$, $\bar{\mu}_2$	first ordinary and second central moments of impulse response signal, respectively
$(\mu_1')_0$, $(\mu_2)_0$	moments of tracer inlet pulse
$(\mu_1')_d$, $(\mu_2)_d$	moments of dead volumes
$(\mu_1')_{0d}$, $(\mu_2)_{0d}$	combined moments of inlet pulse and dead volumes

REFERENCES

1. Kubín M.: Collect. Czech. Chem. Commun. *30*, 1104, 2900 (1965).
2. Kučera E.: J. Chromatogr. *19*, 237 (1965).
3. Schneider P., Smith J. M.: AIChE J. *14*, 762 (1968).
4. Wakao N., Kaguei S., Smth J. M.: J. Chem. Eng. Jpn. *12*, 481 (1979).
5. Fahim M. A., Wakao N.: Chem. Eng. J. *25*, 1 (1982).
6. Wakao N., Tanaka K.: J. Chem. Eng. Jpn. *6*, 338 (1973).
7. Wiedeman K., Radeke K.-H., Gelbin D.: Chem. Tech. (Berlin) *28*, 590 (1976).
8. Carleton F. B., Kersenbaum L. S., Wakeham W. A.: Chem. Eng. Sci. *33*, 1239 (1978).
9. Pazderník O., Schneider P.: J. Chromatogr. *207*, 181 (1981).

Translated by the author (P.S.).